

**S1-5-6**

## Development of Thermally Adaptive ECC for Passive Building Envelope Heat Storage

Devki DESAI

*Graduate School of Civil Engineering, University of Michigan, USA*

Meredith MILLER

*School of Mechanical Engineering, University of Michigan, USA*

Jerome P. LYNCH

*Associate Prof., Dept. of Civil Engineering, University of Michigan, USA*

Victor C. LI

*Professor, Dept. of Civil Engineering, University of Michigan, USA*

### ABSTRACT:

To provide passive heat storage in buildings, materials exhibiting a phase-change within building operating temperature can be incorporated into the envelope material. This study assesses the viability of incorporating a paraffin phase change material (PCM) into an Engineered Cementitious Composite (ECC). ECC allows formation of thin panels—a favorable geometry for building façades. Inclusion of 3% PCM by mass provided a 40% increase in ECC heat capacity at phase change temperature while maintaining a 28 MPa compressive strength, and 4% tensile strain capacity on average.

**Keywords:** Phase-change material, Engineered Cementitious Composite, passive heat storage

### 1. INTRODUCTION

Approximately 40% of home energy use, the greatest percentage in comparison to other uses, is dedicated to space heating and cooling in the United States [1]. However, much of this energy is ultimately lost through the building envelope. Thus, in the field of building design, much effort has been dedicated to considering passive heat storage strategies such as roof ponds and thermal storage walls [2]. A common theme amongst many of the design strategies is utilization of high thermal mass in the building envelope to store heat during the warmest segment of the day and re-radiate the heat into the building as the ambient temperature cools. This can flatten daily temperature fluctuations experienced indoors.

High thermal mass in a building component can be achieved by increasing the mass of material used or by increasing the specific heat capacity of the material. As concrete is a ubiquitous façade material, this study focuses on the feasibility of increasing its specific heat capacity so that the thermal mass in concrete envelopes can be increased without increasing the mass of concrete used.

One manner of increasing the heat capacity of a composite material is introducing a component which undergoes a phase change within building operating temperature. This is because as a material undergoes a phase change from solid to liquid, heat is consumed

to break chemical bonds. The opposite occurs as the material resolidifies; it releases heat to its surroundings as bonds reform [3]. This provides a passive means of heat storage within the material.

There are a number of phase change materials (PCMs) which have been considered for integration into building components such as hydrated salts, fatty acids and paraffins. A relative advantage provided by paraffin waxes is the availability of paraffins with melting points around indoor comfort temperature and their low thermal conductivity [3]. The latter lends an insulative effect in addition to the thermal storage of phase change.

Paraffin PCM has thus far been successfully incorporated into self-compacting concrete [4]. The type of concrete chosen as the matrix for the paraffin PCM in this study is an Engineered Cementitious Composite (ECC). ECC was chosen due to its potential to be cast into thin panels for building envelopes without the need for reinforcing bars. ECC can also be made pigmentable [5]. This can allow for much creativity in geometry, color, and adjustment of surface reflectivity. Further, ECC can be used as a façade or structural material due to its compressive strength and tensile ductility [6].

The components of ECC include cement, fly ash, fine aggregate and fiber reinforcement, often polymer fiber. The mix proportions are dictated by

Table 1. PCM-ECC batch proportions. All proportions provided as mass with respect to cement content.

Batch Name	Type 1 Cement	Fly Ash (Class F)	Sand (F-110)	Water	Superplasticizer*	PVA fiber**	PCM dispersion
0% PCM-ECC	1	2	1.11	0.79	0.02	0.06	0.00
3% PCM-ECC	1	2	1.11	0.67	0.02	0.06	0.36

\*ADVA 405 from W.R. Grace.

\*\*12mm in length with a 40 micron diameter and a 1.2% oil coating.

micromechanical principles in order to achieve the optimal balance between parameters such as matrix toughness and fiber-matrix bond, allowing the concrete to provide tensile strength and ductility as well as compressive strength [6].

The aim of this study is to determine whether a microencapsulated paraffin PCM can be incorporated into an ECC mix and deliver a significant improvement in heat capacity and thermal resistance while retaining mechanical integrity.

## 2. MATERIAL DESIGN

### 2.1 Mix Proportions

The materials used in the design of PCM-ECC are type 1 cement, class F fly ash, fine silica sand, water, poly-vinyl alcohol (PVA) fiber, superplasticizer, and a PCM dispersion. The PCM dispersion contains microencapsulated paraffin wax with a melting point of 23°C.

Two mixes will be discussed in this article: a control 0% ECC mix and a 3% PCM-ECC mix, proportions of which are provided in Table 1. The control mix was created to serve as a matrix conducive to inclusion of PCM, rather than as an optimal ECC design. The 3% PCM-ECC mix incorporates 3% microencapsulated paraffin by mass, and adjusts the water content to account for water added via the dispersion. Discussion of other PCM-ECC mixes created will be included in a more complete report.

The water and superplasticizer content were dictated by the necessary rheology for optimal fiber dispersion in addition to workability requirements. Mini-cone flow rate tests were conducted on the fiberless matrix of all batches tested, and the water and superplasticizer content were adjusted to provide a flow rate of 24-33 seconds as recommended by Li and Li (2012) [7]. It is noteworthy that use of superplasticizer is limited by its ability to cause segregation of matrix components at high concentrations.

It was hypothesized that the addition of PCM would lower the matrix toughness of ECC, lowering the composite compressive and tensile strength. Thus, a

high-activity class F fly ash was utilized to raise the matrix toughness beyond the desired amount in the control mix, and counter-act the hypothesized effect of PCM inclusion in the 3% PCM-ECC mix.

### 2.2 Scanning Electron Microscopy

In order to determine whether the PCM microcapsules were ruptured in the mixing and curing processes, scanning electron microscopic (SEM) images were taken of a cured 3% PCM-ECC specimen. A Quanta 200 3D apparatus was utilized for this process.

Figure 1 provides one such SEM image. It shows numerous PCM capsules which appear to be unruptured by the mixing and curing process. The capsules are 5µm in diameter on average and resemble crumpled spheres prior to addition to the matrix. The capsules seem to retain this geometry within cured ECC.

We can also observe the PCM particles amidst other components of the ECC matrix. Smooth, spherical fly ash particles, 0.2-100 µm in diameter are dispersed throughout. The relief of a buried PVA fiber near the left side of the frame can also be seen, as well as an interconnected system of dark capillary pores.

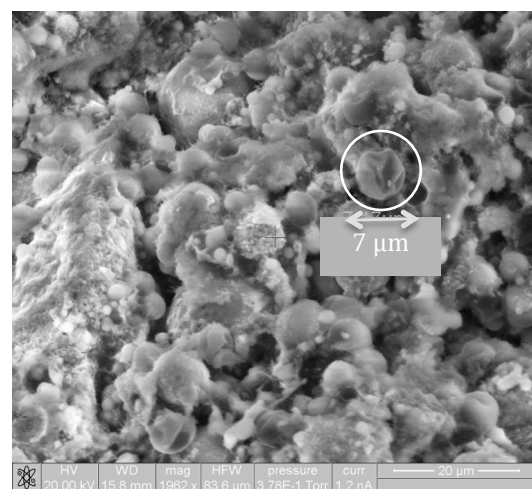


Figure 1. SEM image of a 3% PCM-ECC specimen. Diameter and location of one PCM capsule indicated above.

The SEM imaging process also allows us to observe the distribution of PCM capsules within the matrix. From Figure 1, we can see that the capsules have dispersed rather than clumped. The differential scanning calorimetry results discussed in a subsequent section seem to support this observation.

### 3. MECHANICAL TESTING

#### 3.1 Compressive Strength

The 28-day compressive strength of control (0% PCM) ECC and 3% PCM-ECC were tested using cubes with 50.8 mm sides, testing three cubes per mix design. The results are shown in figure 2. The range of compressive strength attainable with engineered cementitious composites is demarcated in grey for comparison [6].

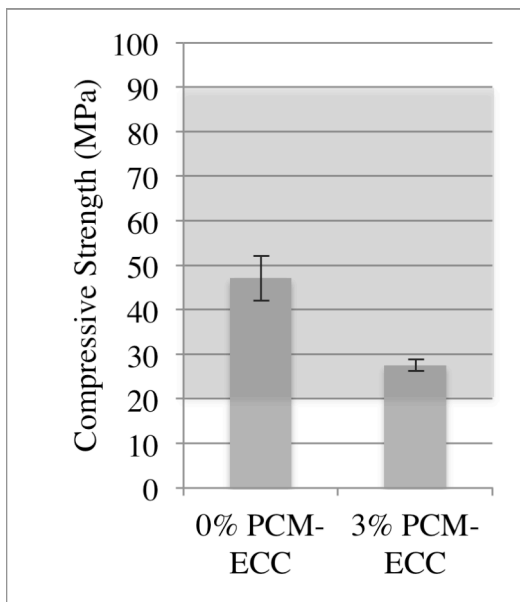


Figure 2. Compressive strength comparison between 0% and 3% PCM-ECC. Shaded region demarcates attainable range with ECC. The 95% confidence intervals are indicated as error bars.

The presence of PCM did lower the compressive strength of the ECC, from 47 MPa to 28 MPa, on average. This is likely due to a decrease in matrix toughness and/or an increase in initial flaw size. These could be caused by poor bonding between the PCM microcapsules and surrounding cement paste, as well as an increase in capillary pores created by the addition of water via the PCM dispersion and due to workability requirements.

According to the Portland Cement Association [8], the lower bound on compressive strength generally

used for structural concrete is 17 MPa. If PCM-ECC is intended for use as a façade panel material, the compressive strength is sufficient, and it also has potential for structural use.

#### 3.2 Tensile Behavior

The availability of tensile strength and strain capacity is a benefit of using an ECC as opposed to conventional concrete. In this study, four dogbone-shaped specimens were cast per mix design and tested accordance with the Japanese Society of Civil Engineers guidelines. The resulting 28-day tensile behavior is presented in figures 3-4. While the first cracking tensile stress was 3 MPa on average for both 0% and 3% PCM-ECC, the behavior differed in terms of ultimate tensile strength, tensile strain capacity and residual crack widths. The presence of PCM reduced the ultimate tensile strength of the ECC from 5.2 to 4.3 MPa, but increased the tensile strain capacity from 2% to 4%.

The increase in tensile strain capacity was likely achieved due to an improved balance between matrix toughness, fiber-matrix bond and other parameters once PCM was added. We can also see from figure 3, the residual crack widths after tensile testing decreased from 60 microns on average to 10 microns once PCM was added to the control mix.

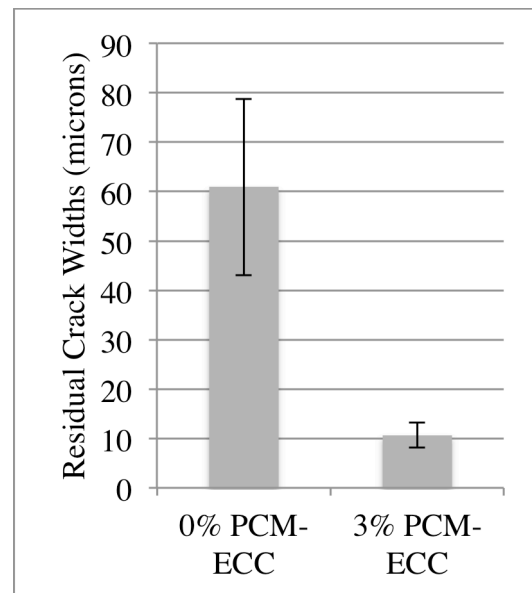


Figure 3. Residual crack widths of 0% and 3% PCM-ECC specimens after JSCE dogbone tension tests were conducted.

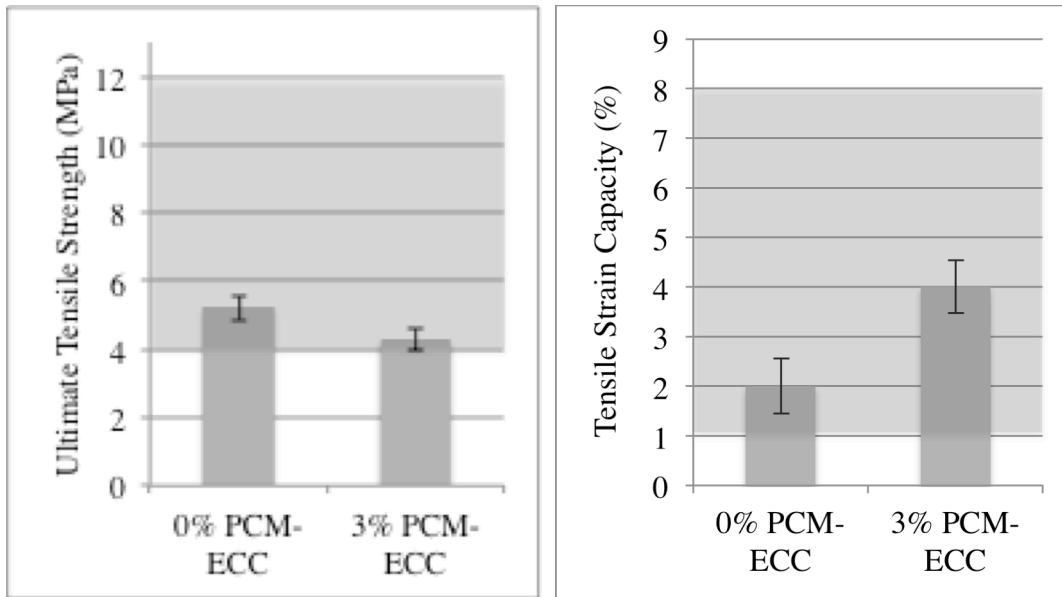


Figure 4. Ultimate tensile strength (left) and tensile strain capacity (right) of 0% and 3% PCM-ECC mixes. Shaded grey area represents range previously attained with various ECC designs [6].

#### 4. THERMAL TESTING

##### 4.1 Differential Scanning Calorimetry

The most important parameter to optimize when designing PCM-ECC is specific heat capacity (SHC), the source of passive heat storage in the material. The SHC of 0% and 3% PCM-ECC was determined in accordance with ASTM E1269-11 *Determining Specific Heat Capacity by Differential Scanning Calorimetry* (DSC) [9]. In this procedure, a small solid sample, 5-30 mg, is heated over the temperature range of interest, the heat flux into the specimen recorded during the process. For this application, all specimens were heated from 10°C to 40°C at a rate of 2°C per minute. Four samples were tested for each ECC design, and the SHC of the mix was calculated as that of the average of the samples, as shown in figure 5.

In accordance with the ASTM standard, a baseline test and a reference test were conducted prior to testing the specimens of unknown heat capacity. The baseline test calls for subjecting an empty aluminum specimen pan to the chosen heating program, the results of which are used to subtract background heat flow from ECC specimen tests. A reference test is then conducted with the same heating rate, on a specimen with a known SHC profile, which in this case was synthetic sapphire. Finally, the test is run on ECC samples, and the heat flow results are compared to those of the reference sample to determine the ECC SHC profile as detailed below [9].

Following ASTM E1269-11 procedure, the first step in data reduction is determining the calorimetric sensitivity function (E). This is necessary if heat flow calibration of the DSC apparatus is not performed prior to every test, but rather at regular servicing

intervals. The value of E is based upon the chosen heating rate (b), the difference between the baseline and sapphire standard heat flux curves (Dst), the mass of the sapphire (Wst), and the specific heat capacity profile of the sapphire standard (Cpst). The following two equations are valid based upon the condition that there is negligible difference in weight between the specimen pans used between tests.

$$E = [b / (60 * Dst)] [Wst * Cpst] \quad (1)$$

The SHC function of the specimen in J/(g\*K) can then be determined using the difference between the baseline and ECC specimen curves (Ds), the weight of the sample (Ws), E and b.

$$Cp(s) = \frac{60 * E * Ds}{Ws * b} \quad (2)$$

The resulting SHC profiles for the ECC control mix and 3% PCM-ECC are provided in figure 5 with solid lines representing the four test average and dashed lines indicating the 95% confidence intervals.

We find that on average, the thermal capacitance of 3% PCM-ECC is roughly 20% higher than that of the control ECC mix. At the phase change temperature of 23°C, the capacitance peak is about 40% higher than the control ECC average and 20% greater than the background value average of PCM-ECC.

It is notable that while the average value of the SHC profile of 3% PCM-ECC varied between samples, as indicated by the confidence intervals, the percent increase in specific heat capacity at phase change did not vary significantly between samples. This suggests that while the local distribution of some composite components might vary, the distribution of PCM capsules remains fairly constant.

Also, the vertical shift between the 0% and 3% PCM-ECC average SHC profiles should be considered in conjunction with their difference in global density. This is particularly important when using the SHC results in thermal modeling procedures, such as that described in the following section. The density of the 0% PCM-ECC and 3% PCM-ECC mixes considered in this study are 1870 kg/m<sup>3</sup> and 1650 kg/m<sup>3</sup>, respectively, on average.

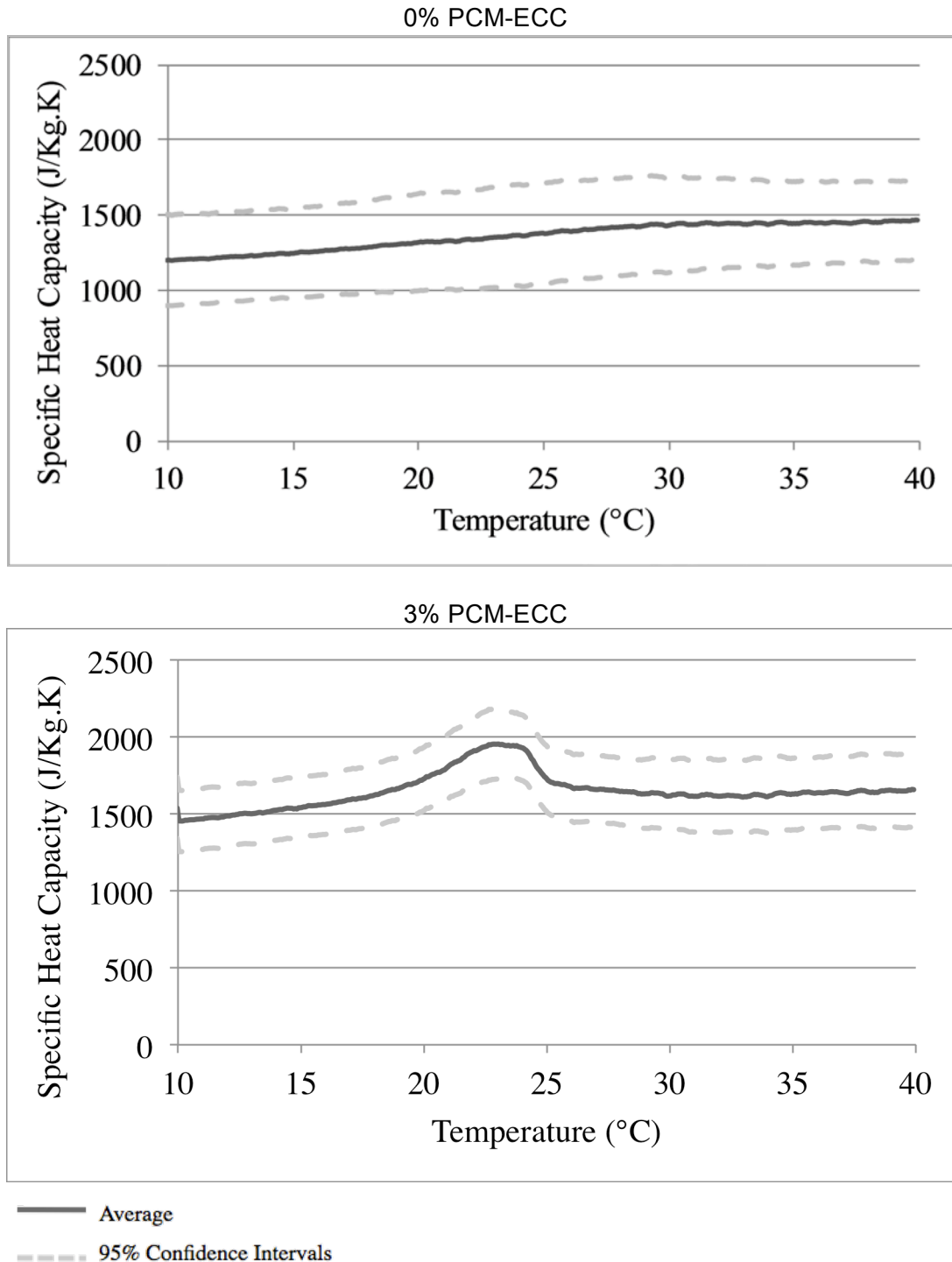


Figure 5. Specific heat capacity profiles of 0% and 3% PCM-ECC as determined by DSC.

#### 4.2 Thermal Resistance

Thermal resistance testing of PCM-ECC was guided by the one-sided experimental setup described in ASTM E2584-07: *Thermal Conductivity of Materials Using a Thermal Capacitance (Slug) Calorimeter* [10]. In this study, a 15 cm x 15 cm x 2.5 cm panel of PCM-ECC was placed between a 15 cm x 15 cm x 1.25 cm steel slug and a heated aluminum plate. As shown in figure 6, the assembly was encased tightly in polystyrene insulation, greater than 2.54 cm in thickness, with an extra 1.3 cm of insulation between the steel slug and apparatus lid. A schematic of thermistor placements is shown in figure 7.

The steel slug is heated from room temperature, approximately 21°C, to 40 °C, by heating the aluminum plate below the PCM-ECC specimen and allowing the heat to propagate upward through the ECC specimen only. This procedure requires approximately 5 hours to run to completion.

Temperature data is recorded by five thermistors placed between the aluminum plate and PCM-ECC specimen and four thermistors placed within longitudinal channels in the steel slug.

Using the specific heat capacity of PCM-ECC determined by DSC, the temperature profile of the heated side of the specimen and that of the steel, as well as the known thermal properties of steel, we can solve for PCM-ECC thermal resistance. The ASTM E2584-07 standard provides an equation to approximate heat-transfer across the specimen and determine this value. Though one can also use the differential equations upon which the ASTM approximation is based to solve for the concrete thermal resistance. Thus, a state space MATLAB model was constructed for this purpose to simulate heat transfer through the assembly based upon the equivalent circuit model shown in figure 8.

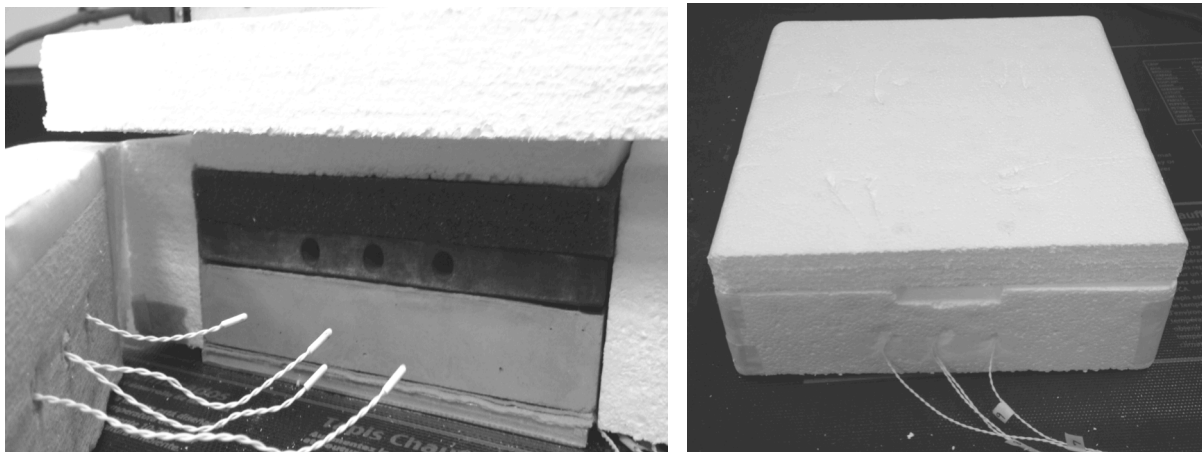


Figure 6. Image of interior of test setup (left) and apparatus during data collection (right).

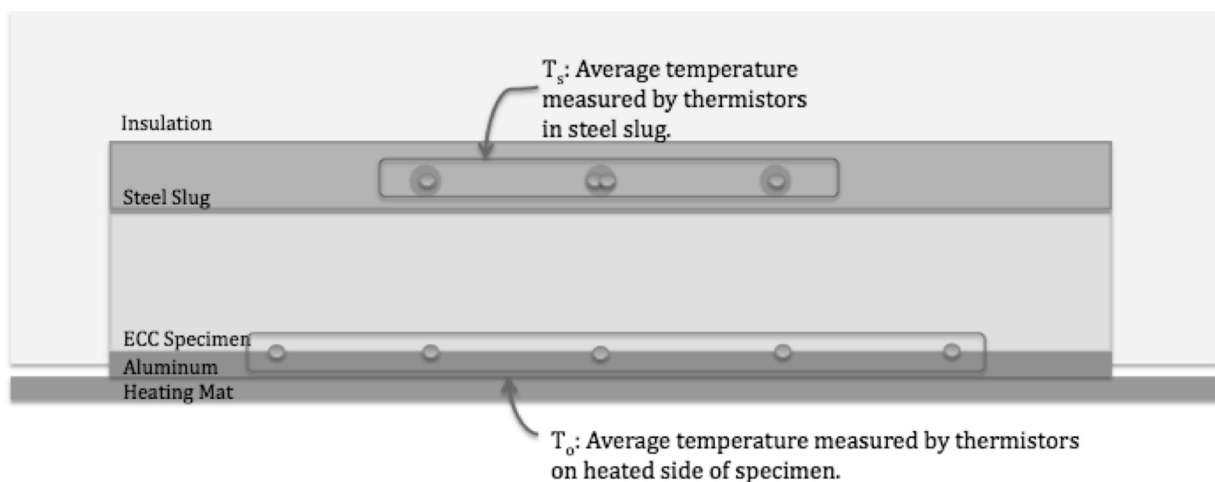


Figure 7. Diagram of thermal resistance test setup.

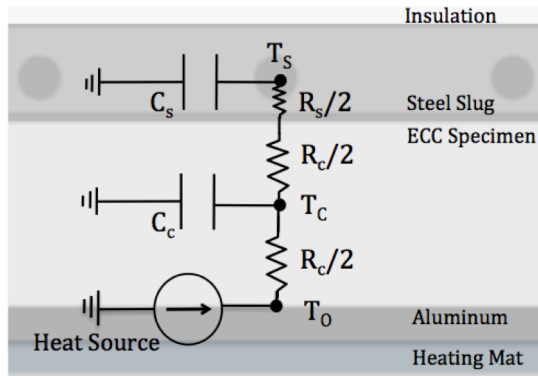


Figure 8. Schematic of equivalent circuit used to model heat transfer through the assembly.

All known material parameters and temperature data were provided to the model. The input temperature,  $T_0$ , is provided by the average value of temperature measured by the five thermistors along the heated side of the ECC specimen, as shown in figure 7. The thermal capacitance of the concrete specimen and the steel slug,  $C_c$  and  $C_s$ , respectively, are obtained by multiplying the specific heat capacity (SHC) of each material by the mass of the material in the experimental setup. The SHC of the steel slug was obtained from the ASTM E2584-07 standard, and the SHC of the ECC specimens were obtained from DSC, as detailed in the previous section. Multiplying the specific resistance of each material by its thickness and dividing by the horizontal cross-sectional area provides the  $R_c$  and  $R_s$  parameters, the thermal resistance of the concrete and slug, respectively. The thermal resistance of the steel slug is obtained from the literature, while the thermal resistance of the concrete specimen is determined as described below.

Since the specific resistance of the PCM-ECC specimen is unknown, the initial value is guessed and thereafter iteratively solved for by minimizing the difference between the program output of the steel slug temperature profile, with the experimental steel slug temperature profile. The matrix of equations (3) is solved in state-space format at each time step, and is graphically represented in figure 8.

$$(3) \quad \begin{bmatrix} \dot{T}_c \\ \dot{T}_s \end{bmatrix} = \begin{bmatrix} \frac{-2}{C_c R_c} & \frac{-2}{C_c (R_c + R_s)} & \frac{2}{C_c (R_c + R_s)} \\ \frac{2}{C_s (R_c + R_s)} & \frac{-2}{C_s (R_c + R_s)} & 0 \end{bmatrix} \begin{bmatrix} T_c \\ T_s \end{bmatrix} + \begin{bmatrix} \frac{2}{C_c R_c} \\ 0 \end{bmatrix} T_0$$

For both 0% and 3% PCM-ECC, the thermal resistance test was performed on three specimens. The resulting thermal resistance, averaged over the temperature range tested, is provided in figure 9.

It can be seen in figure 9 that the thermal resistance of

3% PCM-ECC is higher than that of 0% PCM-ECC. This provides an added benefit to the use of PCM in concrete, as the phase change will delay the propagation of heat through a PCM-ECC envelope component, while the increase in thermal resistance will dissipate heat travelling through the envelope. The former provides latent heat storage, and the latter provides an insulative effect.

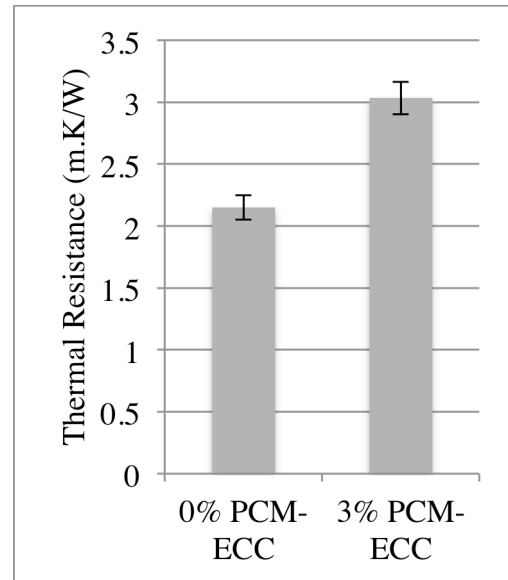


Figure 9. Specific thermal resistance of 0% and 3% PCM-ECC.

### 5. PCM IN BUILDINGS

The effect of PCM on the thermal dynamics of a building depends greatly upon the mass and location of PCM inclusion as well as overall building materials, geometry, and climate. Experimental and numerical studies have been conducted to estimate the energy savings increased thermal mass via phase-change can afford.

An analysis of PCM-concrete enclosures conducted by Cabeza et al. (2007) found that PCM incorporation can reduce peak indoor temperatures by 1-2 degrees Celsius, indicating the increased thermal resistance. The experiment also found that the peak daily temperature of 5% PCM-concrete walls is delayed by 2 hours in comparison to those without PCM [11]. This can help stabilize indoor temperature particularly if applied in a climate with high diurnal temperature fluctuations.

Tabares-Velasco (2012) conducted simulations of PCM within building envelopes. One such simulation incorporated 1.6 kg of PCM per square meter of wall area, with PCM melting temperature set at the upper end of indoor comfort range. The model predicted a 6% annual energy saving and 12% reduction in peak HVAC demand [12].

These findings are relevant to estimation of the effect of PCM-ECC on building thermal performance. In relation to the Tabares-Velasco study, PCM-ECC can provide 1.6 kg of PCM per square meter with an approximately 3.2 cm thick panel. In light of this and Cabeza et al. findings, it can be hypothesized that PCM-ECC panels could noticeably delay and reduce the magnitude of peak indoor temperatures.

## 6. CONCLUSIONS

- (1) Incorporating a phase-change material into an engineered cementitious composite (ECC) increases the specific heat capacity, and therefore the passive heat storage of the composite, particularly at phase change temperature.
- (2) The 3% PCM-ECC exhibits a lower density and higher thermal resistance than 0% PCM-ECC.
- (3) The compressive strength of the 3% PCM-ECC composite is adversely affected by the presence of PCM, but still surpasses the 17 MPa lower limit for structural concrete mentioned by the Portland Cement Association by over 10 MPa.
- (4) The presence of PCM can increase the tensile ductility of PCM-ECC if the background matrix is prepared with a sufficiently high matrix toughness and fiber-matrix bond.
- (5) PCM-ECC is viable, thermally and mechanically, for use as a component to enhance the passive heat storage of building envelopes.
- (6) In light of experimental and numerical studies of PCM within building envelopes, one could anticipate a noticeable reduction in peak HVAC loads if PCM-ECC panels were to be used.

## ACKNOWLEDGEMENT

The researchers express gratitude to Cementos Argos and the University of Michigan for financial support of this project. The authors also thank BASF for supplying the PCM material used in this study. The first author also appreciates the support of a US National Science Foundation Graduate Research Fellowship.

## REFERENCES

1. Center for Sustainable Systems. "Residential Buildings Factsheet," University of Michigan, 2011, Pub. No. CSS01-08.
2. Brown, G.Z., and DeKay, M. "Sun, Wind, and Light: Architectural Design Strategies" (2 ed), New York: John Wiley and Sons, 2001.
3. Baetens, R., Jelle, B.P., Gustavsen, A., "Phase change materials for building applications: A state-of-the-art review," *Energy and Buildings*, Vol. 42, Sept. 2010, pp.1361-1368.
4. Hunger, M., Entrop, A.G., Mandilaras, I., Brouwers, H.J.H., Founti, M., "The behavior of self-compacting concrete containing micro-encapsulated Phase Change Materials," *Cement and Concrete Composites*, Vol. 31, 2009, pp.731-743.
5. Yang, E., Li, V.C., "Development of pigmentable Engineered Cementitious Composites for architectural elements through integrated structures and materials design," *Materials and Structures*, Vol. 45, Mar. 2012, pp. 425-432.
6. Li, V.C. "Engineered Cementitious Composites – material, structural, and durability performance," *Concrete Construction Engineering Handbook*, CRC Press, Ed. E. Nawy, 2008, Ch. 24.
7. Li, M. and Li, V.C., "Rheology, fiber dispersion, and robust properties of Engineered Cementitious Composites," *Materials and Structures*, DOI: 10.1617/s11527-012-9909-z, 2012.
8. Portland Cement Association (PCA), *Concrete Technology*, 2012.  
[http://www.cement.org/tech/faq\\_strength.asp](http://www.cement.org/tech/faq_strength.asp)
9. ASTM Standard E1269-11, "Determining Specific Heat Capacity by Differential Scanning Calorimetry," ASTM International, West Conshohocken, PA, 2011.
10. ASTM Standard E2584-07, "Thermal Conductivity of Materials Using a Thermal Capacitance (Slug) Calorimeter," ASTM International, West Conshohocken, PA, 2007.
11. Cabeza, L.F., Castellon C., Nogues M., Medrano M., Leppers R., Zubillaga O. "Use of microencapsulated PCM in concrete walls for energy savings," *Energy and Buildings*, Vol. 39, Mar. 2006, pp. 113-119.
12. Tabares-Velasco P.C. "Energy impacts of nonlinear behavior of PCM when applied into building envelope," NREL preprint, presented at ASME 2012 6th International Conference on Energy Sustainability & 10th Fuel Cell Science, Engineering and Technology Conference, Aug. 2012.